

Improved Current Regulators for Sensorless Synchronous Reluctance Motor

Abstract. To achieve rapid response, good tracking performance and high efficiency, different types of control strategies have been adopted for synchronous reluctance motors (SynRMs). In this paper, a new approach to rotor speed estimation of a sensorless reluctance synchronous motor is proposed. It consists of replacing the conventional PI current controller with that based on model predictive control (MPC) using the adaptive model reference estimator (MRAS) upstream. The stator current and speed are first estimated by the MRAS technique and then injected into the MPC block to calculate the reference voltage vector (RVV). This new approach which takes into account all the mechanical and electrical variables in a control law via a new cost function allows to obtain the signals switched to the power converter. The overall system is implemented in MATLAB/SIMULINK.

Streszczenie. Aby osiągnąć szybką reakcję, dobrą wydajność śledzenia i wysoką wydajność, przyjęto różne typy strategii sterowania dla synchronicznych silników reluktancyjnych (SynRM). W artykule zaproponowano nowe podejście do szacowania prędkości obrotowej wirnika bezczujnikowego reluktancyjnego silnika synchronicznego. Polega ona na zastąpieniu konwencjonalnego regulatora prądu PI regulatorem opartym na modelowym sterowaniu predykcyjnym (MPC) z wykorzystaniem adaptacyjnego estymatora odniesienia modelu (MRAS). Prąd i prędkość stojana są najpierw szacowane za pomocą techniki MRAS, a następnie wprowadzane do bloku MPC w celu obliczenia wektora napięcia odniesienia (RVV). To nowe podejście, które uwzględnia wszystkie zmienne mechaniczne i elektryczne w prawie sterowania za pomocą nowej funkcji kosztu, pozwala na uzyskanie sygnałów przełączanych do przekształtnika mocy. Cały system jest zaimplementowany w środowisku MATLAB/SIMULINK. (Ulepszone regulatory prądu dla bezczujnikowego synchronicznego silnika reluktancyjnego)

Keywords: Sensorless Control, Synchronous reluctance motor, Model Reference Adaptive System, model predictive control.

Słowa kluczowe: Sterowanie bezczujnikowe, synchroniczny silnik reluktancyjny, modelowe sterowanie predykcyjne, referencyjny

Introduction

SynRMs have a cost advantage as they do not require expensive rare earth elements compared to permanent magnet synchronous motors. They are very tolerant of misuse, as there are no magnets to overheat and demagnetise. The operating principle of these motors is based on the difference in magnetic flux along the direct axis (d-axis) and the quadrature axis (q-axis).

Sensorless control of SynRMs eliminates the need for electrical and mechanical sensors, with the advantages of compact size, lower cost, higher stability, increased noise immunity, greater reliability, a wide range of operations, and reduced maintenance requirements.

Furthermore, sensorless vector control used in synchronous reluctance motors (SynRMs) is becoming a growing trend in industrial applications

The main problems to be solved when dealing with sensorless drives are: motor parameter variations due to magnetic saturation and temperature changes, inductance and resistance of the motor change, computational mathematics used leads to increased reliability of the voltage and current measurements, large variations in load and speed can lead to an erroneous estimate.

Observers such as the Luenberger observer (Bose, 2003), the extended Kalman filter (Hussain et al., 2014) and the unrefined Kalman filter (Hussain et al., 2015; Chan et al., 2009) have been proposed for the estimation of speed in AC drives. Such observers need the accurate mathematical system model for estimation intents and purposes. They are therefore strongly reliant on the parameters of the motor. In addition, the mathematics of the schemes is intensive and needs many adjustments. The most widely used approach in these observer is a synchronous frame proportional-integral (PI) controller often augmented with decoupling terms to compensate for cross-coupling due to the rotating coordinate system [1], [2],[3],[4],[5]-[9]. This control has been widely applied in electric drives and it is estimated that more than 95% of controllers

used in industry are PID controllers, and most of them are PI controllers [10]- [11], [9]. It has good steady-state and transient performance and uses pulse width modulation (PWM) to generate the voltages required by the motor.

The weakness of this control scheme is the employment of multiple PI controllers in the outer and inner loops, which have numerous parameters to be set, compared to these techniques, we propose an observer that, in addition to estimating the speed by replacing these conventional PI controllers with a predictive control model that calculates the new speed estimate based on the MRAS scheme using only the stator current and voltage measurements, provides an independent resistance control model and improved disturbance rejection capability. The paper is structured in the following manner:

We opted to an MRAS observer due to its less computationally demanding and suitable for practical implementation, the method was initially suggested in [13] and later in [14].

In this paper a functional candidate is introduced which requires only voltage and current information for speed estimation.

MRAS technique is developed to minimize the error between real quantity and an estimated quantity. This is achieved by comparing the results of two flow estimators derived from different formulations [15].

Then the model predictive control (MPC) block is proposed, due to its fast response speed, its ability to achieve multiple nonlinear objectives, and to solve the limitation of bandwidth in sensorless vector control system, the MPC is chosen to meet these requirements, a current controller where firstly designed in the continuous-time domain is discretized for the digital implementation using the Euler approximation [16],[17],[5]- [7] to predict stator currents in the dq reference frame.

Finally, the proposed MRAS-MPC controller is presented as the new approach that takes advantage of the

cost function generated by this approach to obtain the optimal voltage vector that minimizes the current error. The operation of the controller is studied in more detail, the description and justification of the proposed algorithm are presented and its performance is verified by simulations in MATLAB/SIMULINK.

1. Mathematic modelling of SynRM

The SynRM corresponds to a rotating electrical machine with a rotor that doesn't use winding or magnets, instead, this machine has a rotor designed to make use of the reluctance due to its careful design [18],[19],[20]-[21],[22].

$$(1) \quad \begin{cases} V_{ds} = R_s i_{ds} + L_{ds} \frac{di_{ds}}{dt} - \omega_r \phi_{qs} \\ V_{qs} = R_s i_{qs} + L_{qs} \frac{di_{qs}}{dt} + \omega_r \phi_{ds} \end{cases}$$

where: ϕ_{ds} , ϕ_{qs} : Stator flux linkage in the d and q axes, i_{ds} , i_{qs} : Stator current in the d and q axes.

and the flux linkage is given by: (2)
$$\begin{cases} \phi_{ds} = L_{ds} i_{ds} \\ \phi_{qs} = L_{qs} i_{qs} \end{cases}$$

where L_{ds} , L_{qs} : d and q-axes stator inductance

$$(3) \quad \begin{bmatrix} V_{ds} \\ V_{qs} \end{bmatrix} = \begin{bmatrix} R_s & -L_{qs}\omega_r \\ L_{ds}\omega_r & R_s \end{bmatrix} \begin{bmatrix} i_{ds} \\ i_{qs} \end{bmatrix} + \begin{bmatrix} L_{ds} & 0 \\ 0 & L_{qs} \end{bmatrix} \frac{d}{dt} \begin{bmatrix} i_{ds} \\ i_{qs} \end{bmatrix}$$

In the above equations, the speed ω_r is linked to the torque by the mechanical dynamic equation,

$$(4) \quad J \frac{d\omega}{dt} = (T_e - T_r) - f\omega$$

where the angular velocity $\omega = \frac{d\theta}{dt}$, $\omega_r = p\omega$, p : Number of poles; f : Friction coefficient, J : Moment of inertia, T_e : Electromagnetic Torque and T_r : Resistant Torque.

The SynRM state model in d-q is finally written as follows:

$$(5) \quad \frac{d}{dt} \begin{bmatrix} i_{ds} \\ i_{qs} \\ \omega \\ \theta \end{bmatrix} = \begin{bmatrix} -\frac{R_s}{L_{ds}} i_{ds} + \omega_r \frac{L_{qs}}{L_{ds}} i_{qs} \\ -\frac{R_s}{L_{qs}} i_{qs} - \omega_r \frac{L_{ds}}{L_{qs}} i_{ds} \\ \frac{3}{2} \frac{p(L_{ds} - L_{qs}) i_{ds} i_{qs}}{J} - \frac{f}{J} \omega - \frac{T_r}{J} \\ \omega \end{bmatrix} + \begin{bmatrix} \frac{1}{L_{ds}} & 0 \\ 0 & \frac{1}{L_{qs}} \\ 0 & 0 \\ 0 & 0 \end{bmatrix} \begin{bmatrix} v_{ds} \\ v_{qs} \end{bmatrix}$$

The system of equation (5) is non-linear because of the products between currents (i_{ds}, i_{qs}), and speed ω . However, in most cases the mechanical time constant is large relative to the electrical time constants so that the two subsystems, electrical and mechanical, can be considered decoupled. Thus, the speed is considered no constant during the transient regimes.

Figure.1 presents the SynRM model in synchronous reference frame with inputs stator voltages, and load torque. The outputs are the rotor angular velocity

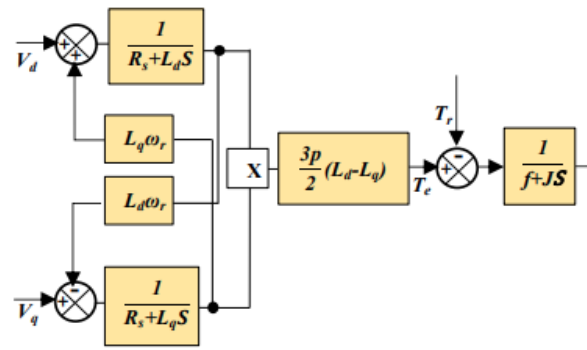


Fig. 1. Block diagram of the SynRM system

2. Mras observer design

MRAS is one of the popular and efficient speed estimation systems applied to motor drives, employed in motor control applications for monitoring and observing the parameters and states of the system. In a MRAS, an adjustable model and a reference model are connected in parallel. For the SynRM motor, the stator currents and voltages are utilized in this speed estimation scheme as shown in Figure 2.

The adaptation laws adjust the estimated speed according to the outputs of the reference and adjustable models. Thus, the MRAS in this model is comparing the outputs of a reference model and an adjustable model, and dealing with the error between these two models on the basis of appropriate adaptive laws that do not affect in any manner the applied system's stability [23], [14]. An essential concern in MRAS is the conception of adaptive laws. The Lyapunov stability and the Popov hyper stability theory have been used as the default design methods to obtain a secure stable adaptive system.

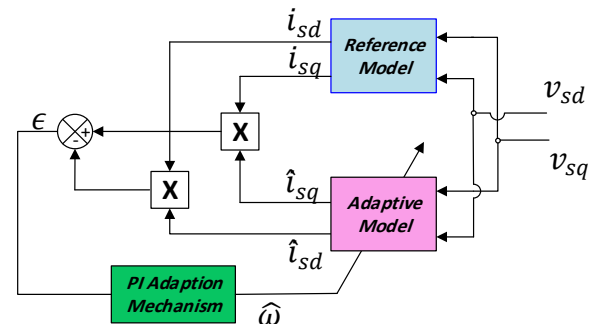


Fig. 2. Structure of MRAS Based Speed Estimator

The SynRM dynamic model can be further adjusted from the model state equation (5) and the adjustable SynRM model can be written:

$$(6) \quad \frac{d}{dt} \begin{bmatrix} \hat{i}_{ds} \\ \hat{i}_{qs} \end{bmatrix} = \begin{bmatrix} -\frac{R_s}{L_{ds}} & \hat{\omega}_r \\ -\hat{\omega}_r & -\frac{R_s}{L_{qs}} \end{bmatrix} \begin{bmatrix} \hat{i}_{ds} \\ \hat{i}_{qs} \end{bmatrix} + \begin{bmatrix} \frac{1}{L_{ds}} & 0 \\ 0 & \frac{1}{L_{qs}} \end{bmatrix} \begin{bmatrix} v_{ds} \\ v_{qs} \end{bmatrix}$$

The following state error equations are obtained by subtracting (5) which applies to the adjustable model from the reference model equations:

$$(7) \quad \frac{d}{dt} \begin{bmatrix} e_d \\ e_q \end{bmatrix} = \begin{bmatrix} -\frac{R_s}{L_{ds}} & \omega_r \\ -\omega_r & -\frac{R_s}{L_{qs}} \end{bmatrix} \begin{bmatrix} e_d \\ e_q \end{bmatrix} - J(\omega_r - \hat{\omega}_r) \begin{bmatrix} \hat{i}_{ds} \\ \hat{i}_{qs} \end{bmatrix}$$

where, $e_d = i_{ds} - \hat{i}_{ds}$, $e_q = i_{qs} - \hat{i}_{qs}$, $J = \begin{bmatrix} 0 & -1 \\ 1 & 0 \end{bmatrix}$

Equation (7) can be represented as ;

$$(8) \quad \dot{[e]} = [A][e] - [\omega]$$

Where ;

$$[\omega] = (\omega - \hat{\omega}) \begin{bmatrix} -\hat{i}_{qs} \\ \hat{i}_{ds} \end{bmatrix} \text{ is the feedback block.}$$

On the forward block, figure 3-a, the term $[\omega]$ is the input and $[e_\omega]$ is the output.

With the simplified boundary condition $[e(\infty)]T=0$ for any initialisation [24],[12], the asymptotic behaviour of the adaptation mechanism is realised. Therefore, the system is hyperstable when the transfer matrix of the direct path is written as follows:

$$(9) \quad G(S) = (SI - A)^{-1}$$

can be verified which is strictly positive real.

In the nonlinear feedback block, the input and output satisfy the Popov criterion [14]:

$$(10) \quad \int_0^t [e]^T [\omega] dt \geq -\gamma^2 \text{ for all } t \geq 0$$

Whith ,

$$(11) \quad [e]^T [\omega] dt = (e_d \hat{i}_{qs} - e_q \hat{i}_{ds})(\omega_r - \hat{\omega}_r)$$

Where γ is positive real constant.

Shauder [14] suggests that the Popov criterion is respected by the adaptation law. It is expressed by the equation:

$$(12) \quad \hat{\omega}_r = \left[\partial_2(e) + \int_0^t \partial_1(e) dt \right]$$

Substituting $[e]$ and $[\omega]$ values, equation 11 becomes:

$$(13) \quad \int \left\{ \left[e_d \hat{i}_{qs} - e_q \hat{i}_{ds} \right] \left[(\omega_r - \partial_2(e)) - \int_0^t \partial_1(e) dt \right] \right\} dt \geq -\gamma^2$$

This inequality can be solved using the following well-known relation:

$$(14) \quad \int_0^t k(f(t))f(t) dt \geq -\frac{1}{2}kf(0)^2, k > 0$$

With this expression, Popov's inequality can be demonstrated by the functions below:

$$(15) \quad \partial_1 = k_i(e_q \hat{i}_{ds} - e_d \hat{i}_{qs}) = k_i(i_{qs} \hat{i}_{ds} - i_{ds} \hat{i}_{qs})$$

$$(16) \quad \partial_2 = k_p(e_q \hat{i}_{ds} - e_d \hat{i}_{qs}) = k_p(i_{qs} \hat{i}_{ds} - i_{ds} \hat{i}_{qs})$$

With ,

$$(17) \quad \varepsilon = i_{qs} \hat{i}_{ds} - i_{ds} \hat{i}_{qs}$$

The following relation can be derived for the speed estimation:

$$(18) \quad \hat{\omega}_r = K_p \varepsilon + \int K_i \varepsilon dt$$

The estimated rotor speed is used to generate an adaptation design for the MRAS speed observers. We can obtain the adaptive law of the observer by reorganized the MRAS structure diagram in Figure 3.

The state expression is represented as follow:

$$(19) \quad \begin{cases} \dot{e} = Ae + Bu \\ y = B^T e \end{cases}$$

From Figure 3.a, it can be seen that the adaptation mechanism is related to the state error , the transfer function of forward channel can be deduced according to

the state space expression equation (9), $\frac{y(s)}{u(s)}$ as

$$(20) \quad G(s) = \frac{(s + \frac{R_s}{L})(i_{ds}^2 + i_{qs}^2)}{s^2 + 2\frac{R_s}{L}s + (\frac{R_s}{L})^2 + \omega^2}$$

So, its simplified structure diagram can be represented as two blocks of $G(s)$ and PI in series where $\hat{\omega}_r$ is the output and ω_r is the input as in Figure 3-b and because the value of $(i_{ds}^2 + i_{qs}^2) = 1$ for maximum torque per Ampere control strategy. This can get the transfer function of system, $G_c(s)$:

$$(21) \quad G_c(s) = \frac{k(s + \frac{R_s}{L})(s + z)}{s^3 + 2\frac{R_s}{L}s^2 + ((\frac{R_s}{L})^2 + \omega_r^2)s}$$

Where ; $k = K_p$ and $z = \frac{k_i}{k_p}$

This can therefore be employed to tune the PI controller parameters with the method of root locus analysis as simplified as the structure diagram in Figure 4, making the system reach the intended result. The design of K_p and K_i is introduced to achieve MRAS stability, tracking errors, and more robust operation.

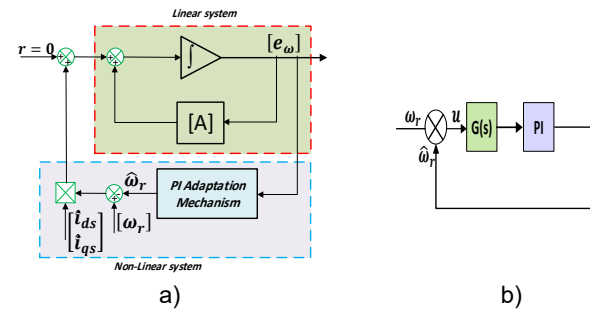


Fig .3. MRAS simplified structure diagram

Adaptive PI controller design criteria is achieved with the use of the root locus method by taking the transfer function of the plant and setting the time domain constraint Figure 4.

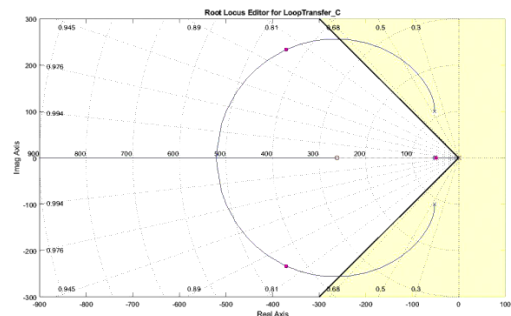


Fig .4. Root locus of closed loop adaptive control system

The constraint taken into account in this design is the percentage overshoot, the settling time and the rise time which are respectively less than 2.09%, 0.0583 seconds and 0.00502 seconds. Therefore, 'z' is taken of 165 and from the root locus diagram of $G_c(s)$ in Figure 4 the maximum possible gain of 'k' should be obtained from the specifications of settling time, maximum

overshoot and rise times of the specification. In this case $K_i = 47258$ then the value of K_p should become 286.41.

As shown in Figure 4, the stator current-based MRAS speed estimator's closed-loop transfer function has all its poles in the left half of the s-plane and therefore, the system has been stable in the operating point. Figure 5 shows the SynRM block diagram based on the FOC (Field Oriented Control) scheme employed in this work.

The principal idea by which the FOC is implemented is the employment of a suitable coordinate system that permits decoupled control of the electrical torque T_e and the rotor flux magnitude $|\phi_r|$. This is realized through aligning the coordinate system to the rotor flux [25],[26].

The motor model is first transformed into d-q components through the α - β to d-q transformation. This transformation requires the rotor speed angle which is estimated as shown in the block of MRAS speed observer [26].

In addition, the MRAS scheme operates as a feedback sensor similar to the shaft position/speed sensor. It can calculate the angular speed of the rotor and generate the angular position of the rotor integrating the angular speed [27].

The estimated motor speed is differentiating with the desired speed. Then it is sent to PI controller. Its purpose is to generate torque reference based on the speed differences, where $i_{qs(ref)}$ is the reference current derived from the torque control loop and $i_{ds(ref)}$ is derived from the rotor flux control loop. The components i_{ds} and i_{qs} are in comparison with the references $i_{ds(ref)}$ and $i_{qs(ref)}$. The current controller outputs are $V_{ds(ref)}$ and $V_{qs(ref)}$, furthermore applied to an inverse Park transformation and used to produce $V_{\alpha s(ref)}$ and $V_{\beta s(ref)}$ based on the position of the rotor speed, which are stator vector voltage components in the stationary orthogonal reference frame. They represent the inputs to the space vector PWM.

This block's outputs are the signals that control the three-phase inverter's power circuit, which turns electrical energy from direct current (DC) into alternating current (AC) [28], [29]. In this case, the voltage that keeps the current error to a minimum is set to 110 volts and the appropriate switching status signals are produced at $t=0.1ms$.

The PWM signals which is finally fed into a controlled inverter to provide required three phase voltage to power the motor under different operating conditions.

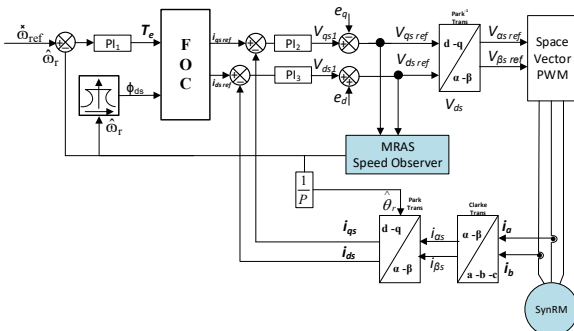


Fig .5. The sensorless vector control of SynRM

The use of Clarke transformation is to convert the 3-Phase stator currents measured into a two phase. This projection's outputs are denoted by i_{α} and i_{β} , when the Park's transformation rotates α - β axis to d-q currents (i_{ds} and i_{qs}) with the reference frequency.

3.Strategy of predictive model

3.1. Predictive design

Predictive control differs from other control techniques in that it has to be solved online, and optimises the predicted future behaviour of a system based on its inputs/outputs. The prediction is made from an inherent model of the system over a time interval called the prediction horizon [30].

The resolution of the optimisation problem is a control vector with the first input of the optimal sequence being sent to the system. The problem is once again solved over the next time interval using the updated system data.

For a sampling time T_s and using the Euler approximation [17] of the stator current derivatives, the predictive motor model (5) will be discretised, this means that:

$$(22) \quad \frac{di}{dt} \approx \frac{i(k+1) - i(k)}{T_s}$$

The stator current equations in the reference frame dq are extracted from (1) and (2):

$$(23) \quad \begin{cases} i_{ds}^p(k+1) = (1 - \frac{R_s T_s}{L_{ds}})i_{ds}(k) + T_s \omega_r i_{qs}(k) + \frac{T_s}{L_{ds}} v_{ds} \\ i_{qs}^p(k+1) = (1 - \frac{R_s T_s}{L_{qs}})i_{qs}(k) - T_s \omega_r i_{ds}(k) + \frac{T_s}{L_{qs}} v_{qs} \end{cases}$$

These equations are used to calculate the stator current predictions for the eight different switching states, denoted by $V_0 - V_7$, and their associated voltage vectors in the stationary reference frame $\alpha\beta$ using a DC voltage V_{dc} , with the six inverter switches named $S_a \dots S_c$ produced by the well-known three-phase inverter with two voltage sources which is connected to the SynRM. After that, the Park transformation is introduced to transform the stator voltages into the dq rotation frame as in [31].

3.2. Setting mpc block

The MPC block is an interactive tool for designing MPC controllers. It is implemented as part of the Model Predictive Control Toolkit. An MPC problem is formulated as a quadratic programming (QP) problem that attempts to minimize a quadratic cost function. MPC computations become more complex as the number of states, constraints, order length and prediction horizons increase. To reduce the complexity and computational time of the MPC in order to run it faster, we apply model order reduction techniques that are used to discard states that do not contribute to the dynamics of the system and use a shorter control and prediction horizon.

All MPC does online is finding the region in which the current state lies and evaluate the linear function to create the current control action. Reducing the iterative optimisation process to the evaluation of the linear function greatly simplifies the runtime calculations. To ensure that a solution is found within the sampling time and that there is even some extra time left for other tasks that need to be executed on the computer. To address this, we determine a maximum value for the number of optimisation iterations.

MPC uses a plant model to make predictions and an optimizer to find the optimal control action, we can specify MPC design parameters for the prediction and control

horizons, and then we see how the system behaviour changes for a larger prediction horizon, then we will play with the control horizon by increasing it to 3 to get better control, after setting all these parameters we can fine tune our controller using the slider, we will drag it to the right for more aggressive control and once the response looks good, we export the controller which updates the MPC controller block and runs the simulation.

4. The proposed Mras-Mpc controller

The remarkable efficiency and price/performance ratio that PID controllers enjoy is still difficult to match. However, this type of controller does not cover all needs and their performance suffers in a certain field of applications such as non-linear, instability, non-stationary, and pure high delay. These limitations have favoured the emergence of predictive control based on digital models. These digital controllers are more capable of algorithmic processing, integrating calculation and logic, than purely analogue controllers

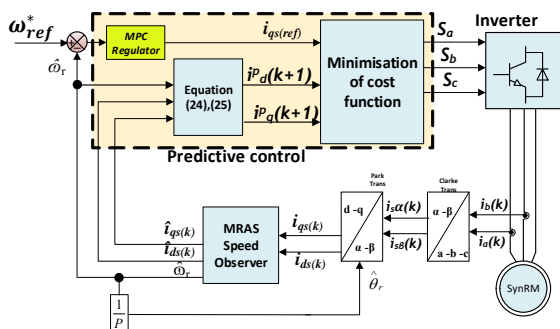


Fig. 6. The proposed MRAS-MPC controller

Figure 6 shows the proposed MRAS-MPC for SynRM; the PI speed controller to generate the torque producing reference current i_q to be injected with the currents i_d and i_q which are subject to predictive control is replaced by the bloc MPC, the currents estimated by the MRAS technique are used in the prediction model to improve the robustness of the proposed method. These current vectors are evaluated by a cost function, that will find the optimum voltage vector that minimises the current error.

The vector voltage can be calculated using (1), (2) :

$$(24) \quad \begin{cases} V_{ds,ref}(k) = R_s \hat{i}_{ds}(k) + L_{ds} \left(\frac{i_{ds,ref}(k+1) - \hat{i}_{ds}(k)}{T_s} \right) - \hat{\omega}_r(k) L_{qs} \hat{i}_{qs}(k) \\ V_{qs,ref}(k) = R_s \hat{i}_{qs}(k) + L_{qs} \left(\frac{i_{qs,ref}(k+1) - \hat{i}_{qs}(k)}{T_s} \right) + \hat{\omega}_r(k) L_{ds} \hat{i}_{ds}(k) \end{cases}$$

The expression of the cost function can be defined as follows:

$$(25) \quad g = \left| i_{ds,ref}(k+1) - i_{ds}(k+1) \right| + \left| i_{qs,ref}(k+1) - i_{qs}(k+1) \right| + \begin{cases} 0 & \text{if } \sqrt{i_{ds}(k+1)^2 + i_{qs}(k+1)^2} \leq i_{s,max} \\ \infty & \text{if } \sqrt{i_{ds}(k+1)^2 + i_{qs}(k+1)^2} > i_{s,max} \end{cases}$$

5. Simulation results and discussion

Firstly, the proposed SynRM speed estimation observer has been implemented and applied to the SynRM field-oriented control, the parameters for the SynRM listed in ap-

pendix, a variable speed reference from -100rad/s to 100rad/s has been applied. As seen the conformity of the actual and estimated speed under nominal resistance. -100 rad/s is applied in the beginning until 0.5 second, we keep going on rising speed to -50 rad/s after we change course towards + 100 rad/s in order to apply the load torque at 2 second. To validate the performance of estimation at a low speed, we applied 10 rad/s at 2.5 second that we can see the good convergence of the estimated and the actual speed with respect to the reference speed.

The estimated rotor speed follows very closely the reference and measured values, as shown in Figure 7, where the speed errors are less than 0.01% of the reference values, indicating a good agreement between the estimated and actual speed, as shown in Figure 8, but a disturbance rejection capacity of up to 88% is observed.

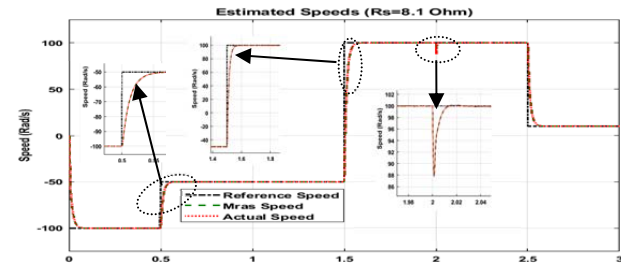


Fig. 7. Estimated Speed with Stator Resistance (R_s) = 8.1

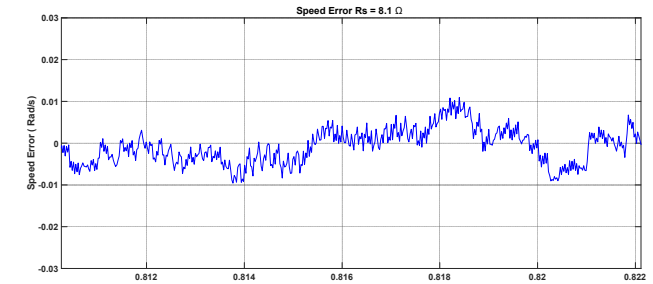


Fig. 8. Zoom speed error $R_s=8.1 \Omega$

The d-q components of the stator currents are shown in Figure 9, i_d maintains its trajectory without significant change until 2.5 seconds, it starts to create short ripples when the speed of 10 rps is applied. Under the influence of the application of load torque at 2 seconds, the current i_q increases from 0 amps to 2.2 amps while still meeting the required operating conditions.

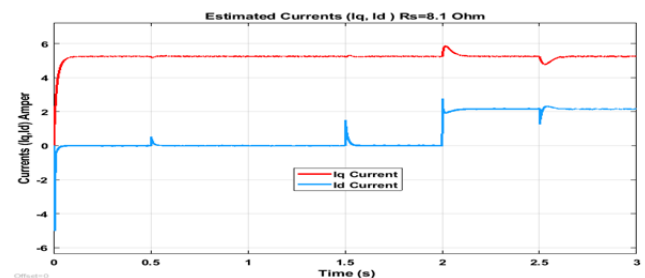


Fig.9. Estimated Currents (I_q, I_d) with Stator Resistance (R_s) 8.1 Ω

From the waveform in Figure 10, each change in reference speed is accompanied by a peak in electromagnetic torque, including at time $t = 2$ seconds when the load torque is applied. At time $t = 2.5$ seconds, small torque ripples are observed at the low speed of 10 radians per second.

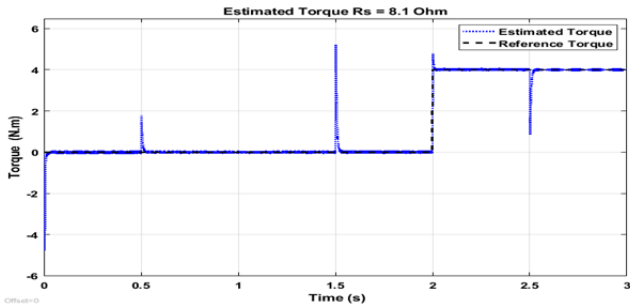


Fig.10. Estimated Torque (Te)with Stator Resistance (Rs)= 8.1 Ω

In order to study against external disturbance, the performances of the new controller and the control system a variation in the stator resistance will be applied, in this test the motor's actual stator resistance is considered to be (18 Ω) more than the motor's nominal resistance (8.1 Ω). Figure 11 shows the comparison of estimated, actual, speed and refer-ence speed, It is clear that the actual and estimated velocities are approximately the same, except that the system response is a little slow and the disturbance rejection is 89%.

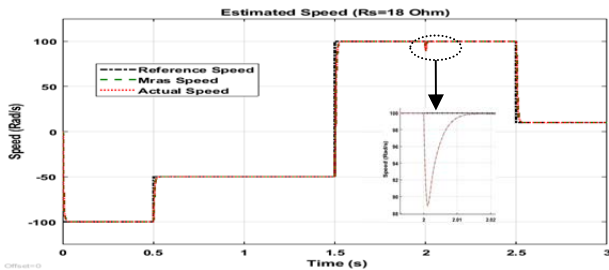


Fig .11. Estimated Speed with Stator Resistance (Rs)= 18

The system was keeping this perfect tracking, when we change the reference speed from -50 rad/s to 100 rad/s, during the speed increasing period we applied the value of 4 Nm of load torque at the moment of 2 seconds, we notice that the speed is not affected by this load torque and continues to follow the applied reference speed 100 rad/s, which means that the robustness of the new controller is achieved.

Although the resistance has been increased up to 18 ohm, the speed remains un-changeable, and has not been affected by this variation as well as noticed on the speed error signal zoom Figure 12, when one can be observed that the range of the error variation does not exceed ± 0.014 rad/s. We can see the rotor speed estimation independence on the resistance, therefore, any variation in the motor parameters would not disturb in the speed estimation. The actual speed is accurately followed by the estimate generated from the new controller.

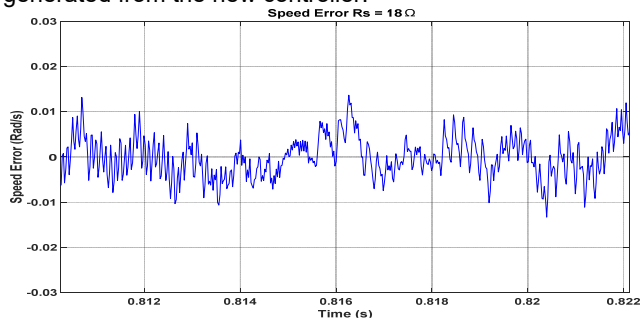


Fig.12. Zoom speed error Rs=18 Ω

In order to test the robustness of the proposed sensorless control scheme, a variation of the load torque from 0 to 4 Nm, as shown in Figure 13, is applied at 2 seconds, based on this information, the influence of the

load variation on the isq current can be observed. The results clearly show that no significant change has been made to the speed or isd current of the machine. The stator current components behave correctly, the id current remains constant, which indicates that decoupling is guaranteed, as shown in figure 13.

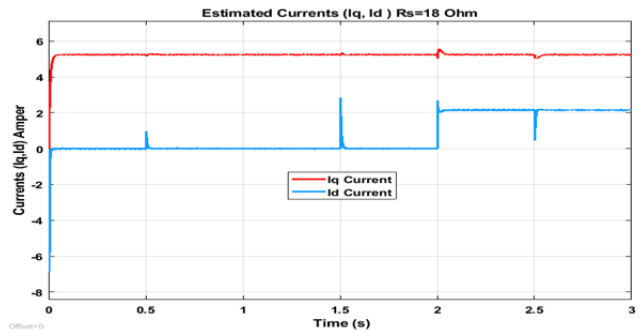


Fig.13. Estimated Currents (Iq, Id)with Stator Resistance (Rs) 18 Ω

The electromagnetic torque is a consequence of iq, so the stator current iq increases as it is directly proportional to the electromagnetic torque, but there are significant torque peaks compared to the nominal resistance condition as illustrated in Figure 14.

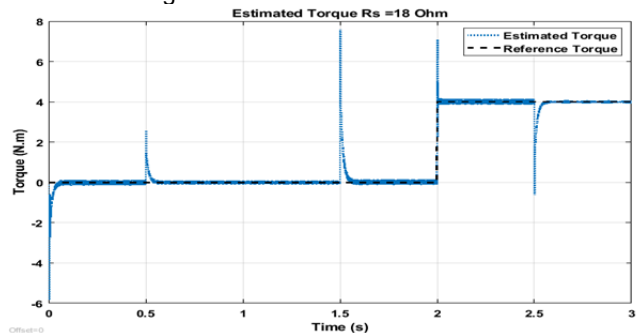


Fig.14. Estimated Torque (Te)with Stator Resistance (Rs)= 18 Ω

All of these tests indicate that the proposed observer controller scheme is robust, more than the current and speed we remain unchanged, so that the uncertainty of the parameters in this process is not greatly affected by the position estimation accuracy.

It can be said, that the resistance parameter variation has no influence on the proposed speed sensorless of SynRM.

Secondly, the proposed SynRM observer using MRAS-MPC method, has been implemented and the specifications generating a valid MPC designer are tested and can be applied. The parameters of the cost function (rate weight of manipulated variable =0.1) and the horizons (prediction horizon =3, control horizon =1) are determined such that the Hessian matrix of the PQ is positively defined. The following table1 lists the controller's minimum MPC parameter along prediction horizon for each manipulated variable (MV) and output variable (OV).

Table 1. Penalty Weights On Manipulated Variable(MV) Rates and Output Variables(OV)

MV(Reference Torque) Weights Rate	OV (Speed) Weights
0.00742736	13.4637

In what follows, for SynRM machine featuring a two-level inverter for which the parameters and ratings are given in Table 3, the steady-state performance of the MRAS-MPC is compared with that of the standard MRAS-

PI. The comparison is made in terms of speed response time, disturbance rejection, torque ripple and stator current. Looking at Figures 15,16,17 and 7,9,10 it can be assumed that the proposed MRAS-MPC has similar performance to that of a conventional MRAS-PI controller. In order to clear up possible misunderstandings, the performance of a MRAS-MPC controller was tested under similar conditions.

Table 2. Comparison results between the different controllers

Controllers	Speed	Torque	Stator currents
PI controller	Good tracking with	increased picks and more ripples	PI controller
New controller with Stator resistance $R_s=18$ Ohm	Good tracking with reject disturbance of 89 % and slow response	increased picks and more ripples	More picks
New controller with Nominal Stator resistance $R_s=8.1$ Ohm	Good tracking with superior disturbance rejection capability (97.5%) and perfect speed ripple reduction	Decreased picks and Less ripples	Decreased picks

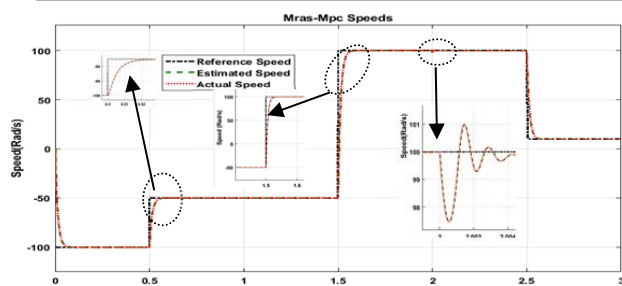


Fig .15. Estimated Speed with New Controller MRAS-MPC

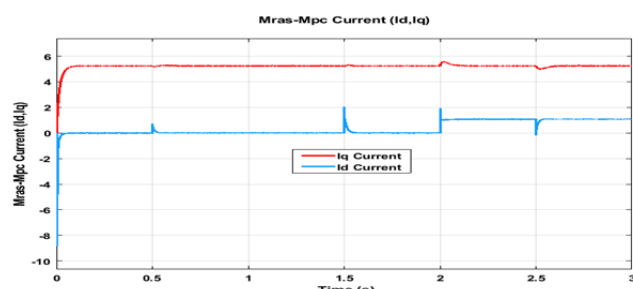


Fig .16. Estimated Currents (I_q, I_d) with New Controller MRAS-MPC

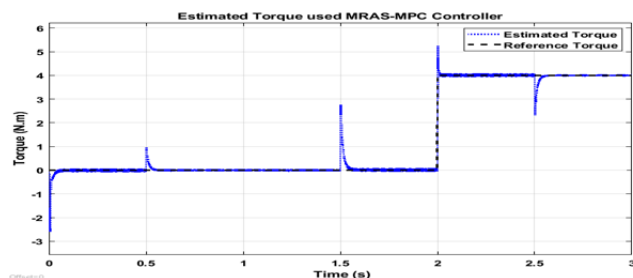


Fig .17. Estimated Torque T_e with New Controller MRAS-MPC

The advantages of this new approach are its superior disturbance rejection capability (97.5%), Figure 15, perfect speed ripple reduction, except for a slight response due to adjusting the state estimation in the MPC toolbox to a

slower mode in order to keep the ripple low, also excellent ripple reduction regarding torque Figure 17, perfect load torque reaction compared to the PI controller, and the stator current components behave correctly with perfect ripple reduction as shown in Figure 16, and to illustrate the performance of this new controller, a recap table 2 is provided below to justify the proposed controller.

Table 3. Parameters of the system used in simulation

d-axis inductance	L_d	0.1524 [H]
q-axis inductance	L_q	0.0345 [H]
Number of poles	p	2
Friction coefficient	f	0.00015 [N.m-1]
Moment of inertia	J	0.00044 [Kg.m ²]
Stator resistance	R_s	8.1 [Ω]
d-time constant	$T_d=L_d.R_s^{-1}$	0.01881 [s]
q-time constant	$T_q=L_q.R_s^{-1}$	0.00426 [s]

6. Conclusion and Future Implications

In this paper, PI speed and current controllers of sensorless synchronous motors are replaced by a predictive control model that calculates the new speed estimate, based on the MRAS scheme, using only the stator current and voltage measurements. The simulation was verified by Matlab/Simulink.

The results of the study show that:

- Under a resistance variation of 8.1 Ohm to 18 Ohm and at very low speed for no-load and on-load conditions, the MRAS-MPC technique is implemented, which shows that the rotor speed estimation is independent of parameter uncertainties and SynRM operating state.

- The estimated quantities are submitted to the MPC block, after the reference current i_q is generated, a cost function takes over this current to provide the inverter with the de-sired switches.

- The predictive control associated with MRAS technique was implemented as a new approach with simulation at a constant speed of 100 rad/s, and an inverter switching of 13.56 MHz, the disturbance rejection capability is greatly improved and the perfect reduction of speed, torque and stator current ripple, an instantaneous reaction of electromagnetic torque to changes in speed and load torque which keeps the system in the right function with respect to that of PI controller.

- The new controller can produce the appropriate voltage to reach the reference speed.

- The simulation results highlighted the performance improvements introduced by this approach.

SynRM's sensorless accuracy estimation performs poorly when the speed is close to zero and the machine parameters need to be studied in more detail, due to voltage measurement noise and integrator drift, although significant progress has been made recently in these areas. Further research is underway in the next study to implement low-pass filters (LPFs) at the input of the MRAS block to reduce torque ripple and pure voltage integration so that they can be implemented in the real world.

Authors: dr. Gati Miloud, El Oued University of Technology, LEVRES Laboratory, Echahid Hamma Lakhdar University of El Oued PB 789, Algeria, E-mail: gati-miloud@univ-eloued.dz; dr. Serhoud Hicham, El Oued University of Technology, Department of Electrical Engineering, Echahid Hamma Lakhdar University of El Oued PB 789, Algeria, E-mail: serhoud-hicham@univ-eloued.dz; dr. Djaghdali Lakhdar University of M'sila, Laboratory of Electrical Engineering, Mohamed Boudiaf University PB 166 M'sila 28000, Algeria, E-mail: djaghdali.lakhdar@univ-msila.dz

REFERENCES

- [1] Shuang, Bo., Z. Q. Zhu., Ximeng Wu., Improved cross-coupling effect compensation method for sensorless control of ipmsm with high frequency voltage injection. *IEEE Transactions on Energy Conversion*, 37 (2021): 347-358.
- [2] Varatharajan, A., Pellegrino, G., Armando, E., Direct flux vector control of synchronous motor drives: Accurate decoupled control with online adaptive maximum torque per ampere and maximum torque per volts evaluation. *IEEE Transactions on Industrial Electronics*, 69 (2021) , 1235-1243.
- [3] Mohammed, Sadeq Ali Qasem., CHOI, Han Ho., JUNG, Jin-Woo., Improved Iterative Learning Direct Torque Control for Torque Ripple Minimization of Surface-Mounted Permanent Magnet Synchronous Motor Drives, *IEEE Transactions on Industrial Informatics*, (2021), vol. 17, no 11, p. 7291-7303.
- [4] Antonello, R., Ortombina, L., Tinazzi, F. ; Zigliotto M., Advanced current control of synchronous reluctance motors, *IEEE 12th International Conference on Power Electronics and Drive Systems (PEDS)*, Honolulu, HI, USA, (2017), 1,037-1,042.
- [5] Accetta, R.A.; Cirrincione, M.; D'Ippolito, F.; Pucci, M.; Sferlazza, A., Input-Output Feedback Linearization Control with On-Line Inductances Estimation of Synchronous Reluctance Motors, *IEEE Energy Conversion Congress and Exposition (ECCE)*, (2021), 4973-4978.
- [6] Hwang, Seon-Hwan, Kim, Jang-Mok, Khang, Huynh Van, al., Parameter identification of a synchronous reluctance motor by using a synchronous PI current regulator at a standstill, *Journal of Power Electronics*, (2010), vol. 10, no 5, p. 491-497.
- [7] Farhan A., Abdelrahem M., Saleh A., Shaltout A., Kennel R., High-Performance Position Sensorless control of Reluctance Synchronous Motor using High-Frequency Injection, *IEEE 13th International Conference on Power Electronics and Drive Systems (PEDS)*, Toulouse, France, (2019), pp. 1-6.
- [8] Altomare A., Guagnano A., Cupertino F., Naso D., Discrete-Time Control of High-Speed Salient Machines, *IEEE Transactions on Industry Applications*, vol. 52, no. 1, (2016), pp. 293-301.
- [9] Lin C K., Yu J t., Lai Y S., Yu H C., Improved Model-Free Predictive Current Control for Synchronous Reluctance Motor Drives, *IEEE Transactions on Industrial Electronics*, vol. 63, no. 6, (2016), pp. 3942-3953.
- [10] Ferdoud, S M., Garcia, Pablo, Oninda., Mohammad Abdul Moin, al., MTPA and field weakening control of synchronous reluctance motor, *9th International Conference on Electrical and Computer Engineering (ICECE)*, (2016). p. 598-601.
- [11] Ghaderi A., Hanamoto T., Wide-Speed-Range Sensorless Vector Control of Synchronous Reluctance Motors Based on Extended Programmable Cascaded Low-Pass Filters, *IEEE Transactions on Industrial Electronics*, vol. 58, no. 6, (2011), pp. 2322-2333.
- [12] Nguyen A T., Rifaq M S., Choi H H., Jung J W., A Model Reference Adaptive Control Based Speed Controller for a Surface-Mounted Permanent Magnet Synchronous Motor Drive, *IEEE Transactions on Industrial Electronics*, vol. 65, no. 12, (2018), pp. 9399-9409.
- [13] Sugimoto H., Tamai S., Secondary Resistance Identification of an Induction-Motor Applied Model Reference Adaptive System and Its Characteristics, *IEEE Transactions on Industry Applications*, vol. IA-23, no. 2, (1987) ,pp. 296-303.
- [14] Schauder C., Adaptive speed identification for vector control of induction motors without rotational transducers, *IEEE Transactions on Industry Applications*, vol. 28, no. 5, (1992), pp. 1054-1061.
- [15] Joo K J., Kim I G., Lee J., Go S C., Robust Speed Sensorless Control to Estimated Error for PMA-SynRM, *IEEE Transactions on Magnetics*, vol. 53, (2017) , no. 6, pp. 1-4.
- [16] Trancho, E., Ibarra, E., Arias, A.; Kortabarria, I.; Jurgens, J.; Marengo, L., Gragger, J. V., PM-assisted synchronous reluctance machine flux weakening control for EV and HEV applications, *IEEE Transactions on Industrial Electronics* ,65, (2017), 2986-2995.
- [17] Clarke G M., Burden R L., Faires J D., *Numerical Analysis*, Cengage Learning, (2012).
- [18] Moghaddam R R., Gyllensten F., Novel High-Performance SynRM Design Method: An Easy Approach for A Complicated Rotor Topology, *IEEE Transactions on Industrial Electronics*, vol. 61, no. 9, (2014) , pp. 5058-5065
- [19] Kolehmainen, J., Synchronous reluctance motor with form blocked rotor, *IEEE Transactions on Energy Conversion*,25, (2010) ,450-456.
- [20] Liu, Y. C., Laghrouche, S., N'Diaye, A.; Cirrincione, M. Hermite neural network-based second-order sliding-mode control of synchronous reluctance motor drive systems, *Journal of the Franklin Institute*,358,(2021), 400-427.
- [21] Peters W., Böcker J., Discrete-time design of adaptive current controller for interior permanent magnet synchronous motors (IPMSM) with high magnetic saturation, *IECON 2013 - 39th Annual Conference of the IEEE Industrial Electronics Society*, Vienna, Austria, (2013),pp. 6608-6613.
- [22] Tornello, L. D., Scelba, G., Scarcella, G., Cacciato, M., Testa, A., Foti, S., Pulvirenti, M., Combined rotor-position estimation and temperature monitoring in sensorless, synchronous reluctance motor drives, *IEEE Transactions on Industry Applications* ,55, (2019), 3851-3862.
- [23] Bu, Y., Wang, A., Design an Improved Sensorless Sliding Mode Observer for PMSM, In *2020 IEEE 3rd Student Conference on Electrical Machines and Systems (SCEMS)*, (2020),100-104.
- [24] Moghaddam R R., Magnussen F., Sadarangani C., A FEM1 investigation on the Synchronous Reluctance Machine rotor geometry with just one flux barrier as a guide toward the optimal barrier's shape, *IEEE EUROCON*, St. Petersburg, Russia, (2009), pp. 663-670.
- [25] Boztas, Gullu., Aydogmus,Omur., Implementation of sensorless speed control of synchronous reluctance motor using extended Kalman filter, *Engineering Science and Technology, an International Journal*, (2022), vol. 31, p. 101066.
- [26] Yousefi Talouki A., Pescetto P., Pellegrino G., Sensorless Direct Flux Vector Control of Synchronous Reluctance Motors Including Standstill, MTPA, and Flux Weakening, *IEEE Transactions on Industry Applications*, vol. 53, no. 4, (2017) , pp. 3598-3608.
- [27] Rodriguez Jose., Patricio Cortes., *Predictive control of power converters and electrical drives*, John Wiley – Sons Book Company (2012)
- [28] Farhan A., Abdelrahem M., Saleh A., Shaltout A., Kennel R., Simplified Sensorless Current Predictive Control of Synchronous Reluctance Motor Using Online Parameter Estimation, *Energies*, vol. 13, (2020), no. 2, p. 492.
- [29] Carlet, Paolo Gherardo., Tinazzi, Fabio., Bolognani, Silverio., al., An effective model-free predictive current control for synchronous reluctance motor drives, *IEEE Transactions on Industry Applications*, vol. 55, no 4, (2019), p. 3781-3790.
- [30] Schwenzer, M., Ay, M., Bergs, T., Abel, D., Review on model predictive control: An engineering perspective, *The International Journal of Advanced Manufacturing Technology* ,117 (2021), 1327-1349.
- [31] Gao X., Abdelrahem M., Hackl C M., Zhang Z., Kennel R., Direct Predictive Speed Control With a Sliding Manifold Term for PMSM Drives, *IEEE Journal of Emerging and Selected Topics in Power Electronics*, vol. 8, no. 2, (2020) ,pp. 1258-1267.